TIME DOMAIN ELECTROMAGNETIC SCATTERING USING FINITE ELEMENTS AND PERFECTLY MATCHED LAYERS

H. T. BANKS AND BRIAN L. BROWNING

Center for Research in Scientific Computation
Box 8205
North Carolina State University
Raleigh, NC 27695-8205
USA

Abstract. We consider a model for the interrogation of a planar Debye medium by a non-harmonic microwave pulse from an antenna source in free space, and we compute the reflected solution using finite elements in the spatial variables and finite differences in the time variable. Perfectly Matched Layers (PMLs) and an absorbing boundary condition are used to damp waves interacting with artificial boundaries imposed to allow finite computational domains. We present simulation results showing that numerical reflections from interfaces at PML boundaries can be controlled.

1. Introduction

The purpose of this paper is to demonstrate computationally that one can implement a two-dimensional version of the electromagnetic interrogation problems introduced in [3]. Here we use perfectly matched layers (PMLs) as absorbing layers at artificial boundaries used to define finite computational domains. We carry out calculations to verify that artificial reflections do not contaminate reflections from dielectric layer interfaces used to determine dielectric parameters as well as physical geometry in inverse problem formulations. Our results provide evidence that the one-dimensional normally incident plane wave ideas in [3] can be extended to treat higher dimensional problems in which obliquely incident waves play a nontrivial role.

In [3] the authors develop a theoretical and computational framework to use pulsed electromagnetic interrogating signals to determine dielectric and geometric properties of materials. This framework involves time domain computations of electromagnetic signals from an antenna through vacuum to the target and return. Even in the one-dimensional case treated in [3] (where one uses an infinite antenna sheet and polarized plane waves to achieve a one-dimensional finite spatial domain), the problems are computationally intensive. Moreover, there are several difficulties in extending this methodology to two and three dimensions in

Date: June 18, 2003.
2000 *Mathematics Subject Classification.* 74J20.
Key words and phrases. scattering, Debye, perfectly matched layers, absorbing boundary condition.

addition to the usual increased computational complexities involved in moving to higher spatial dimensions. First, interrogating signals from a finite antenna will produce oblique incident waves to the target and these must be treated in the reflections. The uniformity assumptions made in [3] to yield one-dimensional finite spatial domains will not be applicable and an infinite spatial domain must be approximated by a finite computational domain with artificial boundaries. Since perfectly absorbing boundary conditions are not available in higher dimensions, some type of boundary damping must be formulated so that artificial reflections will not interfere with reflections from the target.

In the treatment here, we model the propagation of a non-harmonic pulse from a finite antenna source in free space across a planar interface into a dielectric. The dielectric is a Debye medium with Ohmic conductivity. We use finite elements in the spatial variables and finite differences in the time variable to compute the components of the electric field in the case where the signal and dielectric parameters are independent of the y variable (the only uniformity assumption made here). Figure 1 depicts the antenna and dielectric slab geometry we use in our problem formulation with the infinite dielectric slab perpendicular to the z-axis and uniform in the region $z_1 \leq z \leq z_2$. The uniform strip antenna is located in the xy-plane, is infinite in the y-direction and finite in the x-direction lying in the region $-\infty \leq y \leq \infty$, $-\bar{x} \leq x \leq \bar{x}$. An alternating current along the x-direction then produces an electric field that is uniform in y with nontrivial components E_x and E_z depending on (t, x, z) which, when propagated in the xz-plane, results in oblique incident waves on the dielectric surface in the xy-plane at $z = z_1$.

We also assume that the dielectric is backed by a supraconductive material with an infinite conductivity, so one side of the computational domain will have a perfectly reflecting boundary condition. Artificial boundaries on the other three sides are assumed, producing an approximating finite computational domain. Energy will also reflect off the boundaries on these other three sides of the computational domain, and there is a critical need to prevent or delay this energy's return to the domain of interest. We use Perfectly Matched Layers to absorb incident waves without reflection and damp the absorbed waves, and we use a (partially) absorbing boundary condition to limit the amount of energy that reflects off a boundary of the computational domain. When the outgoing wave returns to the domain of interest after twice traversing the PMLs, the wave can be sufficiently attenuated to be negligible when compared to the reflections from the dielectric.

Berenger [5] formulated construction of PMLs for free space using field splitting. Subsequently Sacks et. al. [13] developed the anisotropic formulation for PMLs that we follow here. We formulate the PMLs in terms of auxiliary equations similar to the second order Lorentz equations employed in [3]. (A similar auxiliary equation PML formulation can also be found in [14] and [15].) The absorbing boundary condition we use for PMLs is adapted from Engquist and Majda's first order absorbing boundary condition for free space [10].

A PML can be constructed to match impedance with either free space or a dielectric. Each coordinate axis will determine a one-parameter family of PMLs. The PML parameter determines the degree of energy attenuation in the PML. The parameter domain is $[0, \infty)$, and the PML with parameter 0 corresponds to free space or the dielectric depending on

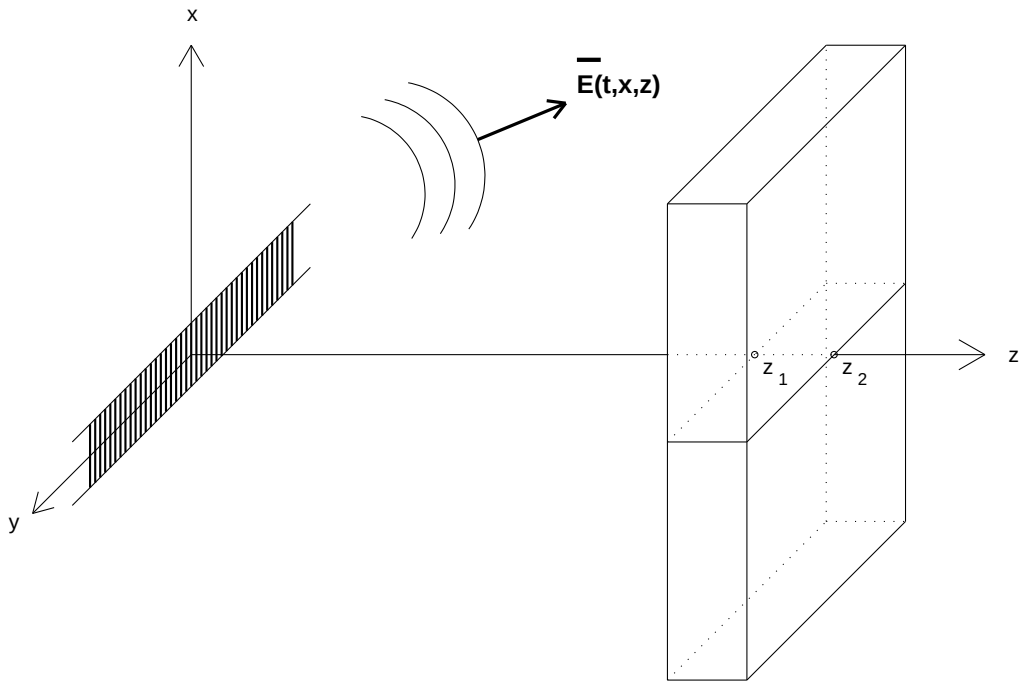

FIGURE 1. Antenna and dielectric material geometry

whether the impedance of the one-parameter PML family is matched to free space or the dielectric. All planar interfaces between two PMLs from the same family will be reflectionless if the interface is normal to the family's coordinate axis. Using one or multiple PMLs from the appropriate family, one can construct a buffer region to a vacuum or to a dielectric that will absorb energy without reflection and then attenuate that energy. In numerical computation there will be reflections at the interfaces between PMLs from the same family, but these reflections can be controlled by making the jumps in the PML parameter sufficiently small. We note that there are relatively few efforts in the research literature on using PMLs with finite elements (see [7] for recent efforts and related references) and, more specifically, with finite antenna generated time domain Maxwell equation propagated fields.

Our research extends the work of Banks, Buksas, and Lin [3] who use finite elements in space and finite differences in time to solve a corresponding one-dimensional forward scattering problem. However, in one dimension, PMLs are not needed since an absorbing boundary condition will absorb all incident energy. For example, if waves propagate at unit speed, the boundary condition $\frac{d}{dz} = \frac{d}{dt}$ at $z = z_0$ absorbs all waves moving in the negative z-direction. There is no reflection since a reflected wave would have the form $f(z - t)$. Unfortunately, absorbing boundary conditions in higher space dimensions will reflect some

energy from all plane waves at non-normal incidence [10]. In our formulation, PMLs provide the necessary extra damping to attenuate the energy that escapes the absorbing boundary condition.

As we have noted above, extending the work in [3] to two dimensions also changes the incidence of the electric field on the vacuum–dielectric interface from normal to oblique incidence. Blaschak and Franzen [6] use Fourier series in the frequency domain to compute the propagation of a time harmonic pulse train of plane waves that enter a dielectric across a planar boundary at oblique incidence. They showed that precursors are excited by short-rise-time pulses at oblique incidence. However, the use of Fourier series restricts this approach to harmonic pulses.

We begin with Maxwell's equations, introduce constitutive relations for a diagonally anisotropic material, and derive the wave equation and its corresponding variational formulation (Section 2). We then compute the reflection coefficient at a planar interface between two diagonally anisotropic materials (Section 3) and find sufficient conditions for a reflectionless interface.

In Section 4 we formulate our problem geometry and the parametrized families of PMLs which we use. We give a single variational equation for the electric field that is valid on the entire computational domain, and we identity differential equations that are satisfied by the polarization and PML terms in the variational equation. A perfectly reflecting boundary condition is applied to the back of the dielectric, and an absorbing boundary condition is applied to the other three sides of the computational domain.

We then discretize our computational domain and derive a finite dimensional system of equations for the electric field (Section 5). We give numerical results in Section 6 which verify that PMLs significantly attenuate energy and that numerical reflections from interfaces at PML boundaries can be controlled.

2. The Wave Equation

To derive the wave equation for a diagonally anisotropic region, we begin with Maxwell's equations for a region with free charge density $\rho = 0$:

$$\begin{aligned} \nabla \cdot \vec{D} &= 0 \\ \nabla \cdot \vec{B} &= 0 \\ \nabla \times \vec{E} &= -\partial_t \vec{B} \\ \nabla \times \vec{H} &= \partial_t \vec{D} + \vec{J}. \end{aligned} \tag{1}$$

The vectors in (1) are functions of position $\vec{r} = (x, y, z)$ and time t. The current density is the sum of a conduction current density and a source current density: $\vec{J} = \vec{J}_c + \vec{J}_s$. We assume only free space can have a source current (e.g., in our antenna), and thus either $\vec{J}_c = \vec{0}$ or $\vec{J}_s = \vec{0}$, depending on whether or not the region is free space.

We next introduce constitutive relations that are sufficiently general to allow for diagonal anisotropy. Let $\mathcal{S}^+$ be the space of tempered distributions on $(-\infty, \infty)$ supported in $[0, \infty)$.

With convolution as multiplication, $\mathcal{S}^+$ is a commutative ring with identity ([11], Sections 5.3, 8.3), and the Dirac delta function δ is the multiplicative identity. Let $\mathcal{M}^+$ be the multiplicative group of invertible elements in $\mathcal{S}^+$, let $C[0,\infty)$ be the space of continuous functions on $[0,\infty)$, and define

$$\mathcal{B}^+ = \{L : L \text{ is a bijection on } C[0,\infty) \text{ and } Lf = g * f \text{ for some } g \in \mathcal{M}^+\}. \tag{2}$$

Observe that $\mathcal{B}^+$ is a group when the binary operator is composition of mappings. In particular $L \in \mathcal{B}^+$ if and only if $L^{-1} \in \mathcal{B}^+$.

Let

$$T = \operatorname{diag}(T_x, T_y, T_z)$$

where T_x, T_y, $T_z \in \mathcal{B}^+$, and let the diagonally anisotropic material's constitutive relations be given by

$$\begin{aligned} \vec{D} &= g * (T\vec{E}) \\ \vec{B} &= \mu_0 T\vec{H} \\ \vec{J}_c &= \sigma T\vec{E} \end{aligned} \tag{3}$$

where $g \in \mathcal{M}^+$, convolution is in the time variable, μ_0 is the permeability of free space, and the constant $\sigma > 0$ is the conductivity. These constitutive relations are sufficiently general to include free space or an isotropic dielectric with Debye model (as well as many other models) for polarization. For instance, if T is the identity operator, $\sigma = 0$, and $g = \epsilon_0\delta$ where ϵ_0 is the permittivity of free space, then (3) describes a vacuum.

Convolution in time commutes with the divergence operator:

$$\begin{aligned} \nabla \cdot \vec{D} &= \nabla \cdot (g * T\vec{E}) \\ &= g * (\nabla \cdot T\vec{E}). \end{aligned}$$

Since $g \in \mathcal{M}^+$ and $\nabla \cdot \vec{D} = 0$ it follows that $\nabla \cdot T\vec{E} = 0$. Let $\mathcal{H}(t)$ be the Heaviside function. Using the constitutive relations (3), we can rewrite Maxwell's equations (1) as

$$\begin{aligned} \nabla \cdot T\vec{E} &= 0 \\ \nabla \cdot T\vec{H} &= 0 \\ \nabla \times \vec{E} &= -\mu_0 T(\partial_t \vec{H}) \\ \nabla \times \vec{H} &= T(\partial_t((g + \sigma\mathcal{H}) * \vec{E})) + \vec{J}_s. \end{aligned} \tag{4}$$

Let

$$\begin{aligned} \widetilde{T} &= (T_x T_y T_z)^{-1} T \\ \widetilde{T}_i &= (T_x T_y T_z)^{-1} T_i \qquad\qquad i = x, y, z. \end{aligned} \tag{5}$$

Then $\widetilde{T} = \operatorname{diag}(\widetilde{T}_x, \widetilde{T}_y, \widetilde{T}_z)$.

We next derive the wave equation for a region Ω where T and g are constant in the spatial variables. Since $\widetilde{T}$ will also be spatially constant in Ω, $\nabla \cdot \widetilde{T}\vec{E} = 0$ by (4). A calculation shows that

$$\begin{aligned} -(\nabla \cdot (\widetilde{T}\nabla))\vec{E} &= -(\nabla \cdot (\widetilde{T}\nabla))\vec{E} + \nabla(\nabla \cdot (\widetilde{T}\vec{E})) \\ &= T^{-1}(\nabla \times (T^{-1}(\nabla \times \vec{E}))). \end{aligned} \tag{6}$$

Consequently using (6) and (4) we obtain

$$\begin{aligned} (-\nabla \cdot (\widetilde{T}\nabla))\vec{E} &= T^{-1}(\nabla \times T^{-1}(\nabla \times \vec{E})) \\ &= -\mu_0 \partial_t T^{-1}(\nabla \times \vec{H}) \\ &= -\mu_0 \partial_t^2((g + \sigma\mathcal{H}) * \vec{E}) - \mu_0 T^{-1}\partial_t \vec{J}_s \\ &= -\mu_0 \partial_t^2(g * \vec{E}) - \mu_0 \sigma \partial_t \vec{E} - \mu_0 T^{-1}\partial_t \vec{J}_s. \end{aligned}$$

Thus the wave equation for $\vec{E}$ in a homogeneous, diagonally anisotropic region Ω with constitutive relations (3) is given by

$$\mu_0 \partial_t^2(g * \vec{E}) + \mu_0 \sigma \partial_t \vec{E} - (\nabla \cdot (\widetilde{T}\nabla))\vec{E} = -\mu_0 T^{-1}\partial_t \vec{J}_s. \tag{7}$$

Define the electric polarization vector $\vec{P}$ by

$$g * E = \epsilon_0 \epsilon_r \vec{E} + \vec{P}$$

where ϵ_r is a relative permittivity that incorporates the instantaneous polarization [3, p.11]. Then the wave equation (7) becomes

$$\mu_0 \epsilon_0 \epsilon_r \ddot{\vec{E}} + \mu_0 \ddot{\vec{P}} + \mu_0 \sigma \dot{\vec{E}} - (\nabla \cdot (\widetilde{T}\nabla))\vec{E} = -\mu_0 T^{-1}\dot{\vec{J}}_s \tag{8}$$

where $\dot{} = \partial_t$ and $\ddot{} = \partial_t^2$. In our problem a current source will exist only in the antenna where T is the identity operator, so the right side of (7) and (8) will reduce to either $\mu_0 \dot{\vec{J}}_s$ or $\vec{0}$.

The components of (8) can be expressed in variational form. Let Ω have piecewise smooth boundary, and let ϕ be a test function on Ω. For a function f on Ω define

$$\langle f, \phi \rangle = \int_\Omega f(\vec{r})\phi(\vec{r})\, dV.$$

If f and ϕ are also defined on $\partial\Omega$ let

$$\langle f, \phi \rangle_{\partial\Omega} = \int_{\partial\Omega} f(\vec{r})\phi(\vec{r})\, ds.$$

We are interested in computing the x-component of $\vec{E}$ which is the signal measured by the finite antenna (see Figure 1) when reflected by the dielectric. Let $\hat{x}$ denote the standard

basis vector parallel to the x-axis, and define

$$\begin{aligned} E &= \vec{E} \cdot \hat{x} \\ P &= \vec{P} \cdot \hat{x} \\ J_s &= (T^{-1}\vec{J}_s) \cdot \hat{x}. \end{aligned} \tag{9}$$

Applying the product rule, the divergence theorem and the definition of $\widetilde{T}$ in (5), we obtain

$$\begin{aligned} \langle (\nabla \cdot (\widetilde{T}\nabla))E, \phi \rangle &= \int_\Omega \nabla \cdot (\phi \widetilde{T} \nabla E)\, dV - \int_\Omega (\nabla \phi) \cdot (\widetilde{T}\nabla E)\, dV \\ &= \int_{\partial\Omega} \phi (\widetilde{T}\nabla E) \cdot \vec{n}\, ds - \int_\Omega (\nabla \phi) \cdot (\widetilde{T}\nabla E)\, dV \\ &= \sum_{i=x,y,z} \langle \partial_i (\widetilde{T}_i E), n_i \phi \rangle_{\partial\Omega} - \sum_{i=x,y,z} \langle \partial_i (\widetilde{T}_i E), \partial_i \phi \rangle \end{aligned}$$

where $\vec{n} = (n_x, n_y, n_z)$ is the outward unit normal to the boundary $\partial\Omega$. Consequently the variational form of the wave equation (8) on Ω is

$$\begin{aligned} \mu_0\epsilon_0 \langle \epsilon_r \ddot{E}, \phi \rangle + \mu_0 \langle \ddot{P}, \phi \rangle + \mu_0 \langle \sigma \dot{E}, \phi \rangle + \sum_{i=x,y,z} \langle \partial_i (\widetilde{T}_i E), \partial_i \phi \rangle - \sum_{i=x,y,z} \langle \partial_i (\widetilde{T}_i E), n_i \phi \rangle_{\partial\Omega} \\ = -\mu_0 \langle \dot{J}_s, \phi \rangle, \end{aligned} \tag{10}$$

or more succinctly

$$\mu_0\epsilon_0 \langle \epsilon_r \ddot{E}, \phi \rangle + \mu_0 \langle \ddot{P}, \phi \rangle + \mu_0 \langle \sigma \dot{E}, \phi \rangle + \langle \nabla \widetilde{T} E, \nabla \phi \rangle - \langle \nabla \widetilde{T} E, \vec{n} \phi \rangle_{\partial\Omega} = -\mu_0 \langle \dot{J}_s, \phi \rangle.$$

Our computational domain will be a region $\mathcal{D}$ that can be partitioned into subregions $\{\Omega_k\}$ with piecewise smooth boundaries such that T and g are constant in the spatial variables on each Ω_k. Consequently, the components of a solution of Maxwell's equations (1) with constitutive relations (3) will satisfy the variational equation (10) on each region Ω_k. Furthermore, the standard interface conditions will be satisfied: $\vec{n} \times \vec{E}$ and $\vec{n} \cdot \vec{D}$ will be continuous across interfaces [2, pp. 13–16].

3. The Reflection Coefficient

To facilitate our use of PMLs in the next section, we compute the reflection coefficient at a typical interface separating two diagonally anisotropic materials. For illustrative purposes, we do this without loss of generality for an interface consisting of the yz-plane at $x = 0$. For this we generalize the calculations in [13]. In the frequency domain, the time harmonic Maxwell's equations in a homogeneous region with no sources and free charge density $\rho = 0$

are

$$\begin{aligned} \nabla \cdot \vec{D} &= 0 \\ \nabla \cdot \vec{B} &= 0 \\ \nabla \times \vec{E} &= -j\omega \vec{B} \\ \nabla \times \vec{H} &= j\omega \vec{D} + \vec{J}_c. \end{aligned} \tag{11}$$

The vectors in (11) are functions of position $\vec{r} = (x, y, z)$ and frequency ω. In the frequency domain the constitutive relations (3) for a diagonally anisotropic material take the form

$$\begin{aligned} \vec{D} &= \epsilon \Lambda \vec{E} \\ \vec{B} &= \mu_0 \Lambda \vec{H} \\ \vec{J}_c &= \sigma \Lambda \vec{E} \end{aligned} \tag{12}$$

where $\epsilon(\omega)$ is the complex permittivity and

$$\Lambda = \operatorname{diag}(\lambda_x, \lambda_y, \lambda_z) \tag{13}$$

is a complex, frequency dependent diagonal matrix.

Let

$$k_0 = \omega \sqrt{\mu_0(\epsilon(\omega) + \sigma/(j\omega))}. \tag{14}$$

Calculations similar to those in Section 2 give the Helmholtz equation for a homogenous, diagonally anisotropic material

$$\left((\lambda_y\lambda_z)^{-1}\partial_x^2 + (\lambda_x\lambda_z)^{-1}\partial_y^2 + (\lambda_x\lambda_y)^{-1}\partial_z^2\right)\vec{E} + k_0^2\vec{E} = 0. \tag{15}$$

Let $\Lambda^- = \operatorname{diag}(\lambda_x, \lambda_y, \lambda_z)$ be the diagonal matrix in the constitutive relations (12) for the region $x < 0$, and let $\Lambda^+ = \operatorname{diag}(\gamma_x, \gamma_y, \gamma_z)$ be the diagonal matrix in the constitutive relations for the region $x > 0$. Take the permittivity ϵ and the conductivity σ to be the same in both regions.

We look for plane wave solutions of Maxwell's equations having the form

$$\begin{aligned} \vec{E}(t, \vec{r}) &= \vec{E}_0 \exp\left(-j(\vec{k} \cdot \vec{r} - \omega t)\right) \\ \vec{H}(t, \vec{r}) &= \vec{H}_0 \exp\left(-j(\vec{k} \cdot \vec{r} - \omega t)\right) \end{aligned} \tag{16}$$

where $\vec{E}_0$, $\vec{H}_0$, and $\vec{k}$ are vectors with complex components, and j is the imaginary unit. Requiring that the plane wave expression for $\vec{E}$ in (16) solve the Helmholtz equation (15) gives a dispersion relation for $\vec{k} = (k_x, k_y, k_z)$ in each region. For $x < 0$

$$(\lambda_y\lambda_z)^{-1}k_x^2 + (\lambda_x\lambda_z)^{-1}k_y^2 + (\lambda_x\lambda_y)^{-1}k_z^2 = k_0^2.$$

For $x > 0$ a similar relation holds with γ replacing λ. The dispersion relation is the equation of an ellipsoid and has solutions

$$\begin{aligned} k_x &= k_0\sqrt{\lambda_y\lambda_z}\cos\theta\cos\phi \\ k_y &= k_0\sqrt{\lambda_x\lambda_z}\cos\theta\sin\phi \\ k_z &= k_0\sqrt{\lambda_x\lambda_y}\sin\theta \end{aligned}$$

where θ and ϕ are complex. In our simulations $E(t,\vec{r})$ will be independent of y, so we take $\phi = 0$ and $k_y = 0$. Let $\hat{x}$, $\hat{y}$, and $\hat{z}$ denote the standard basis vectors. Then for $x < 0$ the incident and reflected wave vectors are

$$\begin{aligned} \vec{k}_i &= k_0\big(\sqrt{\lambda_y\lambda_z}\cos(\theta_i)\hat{x} + \sqrt{\lambda_x\lambda_y}\sin(\theta_i)\hat{z}\big) \\ \vec{k}_r &= k_0\big(-\sqrt{\lambda_y\lambda_z}\cos(\theta_r)\hat{x} + \sqrt{\lambda_x\lambda_y}\sin(\theta_r)\hat{z}\big) \end{aligned}$$

and for $x > 0$ the transmitted wave vector is

$$\vec{k}_t = k_0\big(\sqrt{\gamma_y\gamma_z}\cos(\theta_t)\hat{x} + \sqrt{\gamma_x\gamma_y}\sin(\theta_t)\hat{z}\big). \tag{17}$$

Let TM_y denote a plane wave where $\vec{H}$ has only a y-component, and let TE_y denote a plane wave where $\vec{H}$ has only x- and z-components. Any plane wave can be written as a superposition of TE_y and TM_y waves. Let $\mathcal{R}$ and $\mathcal{T}$ be the reflection and transmission coefficients at the interface for a TM_y wave. Then using a complex parameter A we can express the incident, reflected, and transmitted magnetic fields as

$$\begin{aligned} \vec{H}_i &= \hat{y}\frac{k_0}{\omega\mu_0}A\exp\big(-jk_0(\sqrt{\lambda_y\lambda_z}\cos(\theta_i)x + \sqrt{\lambda_x\lambda_y}\sin(\theta_i)z)\big)\exp(j\omega t) \\ \vec{H}_r &= \hat{y}\frac{k_0}{\omega\mu_0}\mathcal{R}A\exp\big(-jk_0(-\sqrt{\lambda_y\lambda_z}\cos(\theta_r)x + \sqrt{\lambda_x\lambda_y}\sin(\theta_r)z)\big)\exp(j\omega t) \\ \vec{H}_t &= \hat{y}\frac{k_0}{\omega\mu_0}\mathcal{T}A\exp\big(-jk_0(\sqrt{\gamma_y\gamma_z}\cos(\theta_t)x + \sqrt{\gamma_x\gamma_y}\sin(\theta_t)z)\big)\exp(j\omega t) \end{aligned}$$

Calculating $\nabla \times \vec{H}$ using Maxwell's curl equations (11) and the constitutive relations (12), we obtain the electric fields

$$\begin{aligned}
\vec{E}_i &= \left(\sqrt{\frac{\lambda_y}{\lambda_x}}\sin(\theta_i)\hat{x} - \sqrt{\frac{\lambda_y}{\lambda_z}}\cos(\theta_i)\hat{z}\right) \\
&\qquad A\exp\big(-jk_0(\sqrt{\lambda_y\lambda_z}\cos(\theta_i)x + \sqrt{\lambda_x\lambda_y}\sin(\theta_i)z)\big)\exp(j\omega t) \\
\vec{E}_r &= \left(\sqrt{\frac{\lambda_y}{\lambda_x}}\sin(\theta_r)\hat{x} + \sqrt{\frac{\lambda_y}{\lambda_z}}\cos(\theta_r)\hat{z}\right) \\
&\qquad \mathcal{R}A\exp\big(-jk_0(-\sqrt{\lambda_y\lambda_z}\cos(\theta_r)x + \sqrt{\lambda_x\lambda_y}\sin(\theta_r)z)\big)\exp(j\omega t) \\
\vec{E}_t &= \left(\sqrt{\frac{\gamma_y}{\gamma_x}}\sin(\theta_t)\hat{x} - \sqrt{\frac{\gamma_y}{\gamma_z}}\cos(\theta_t)\hat{z}\right) \\
&\qquad \mathcal{T}A\exp\big(-jk_0(\sqrt{\gamma_y\gamma_z}\cos(\theta_t)x + \sqrt{\gamma_x\gamma_y}\sin(\theta_t)z)\big)\exp(j\omega t).
\end{aligned}$$

The tangential components of the total electric and magnetic fields are continuous at the interface $x = 0$. Enforcing this continuity, for example, at the point $(x, z) = (0, 0)$ we have

$$\begin{aligned}
1 + \mathcal{R} &= \mathcal{T} \\
-\sqrt{\frac{\lambda_y}{\lambda_z}}\cos\theta_i + \mathcal{R}\sqrt{\frac{\lambda_y}{\lambda_z}}\cos\theta_r &= -\mathcal{T}\sqrt{\frac{\gamma_y}{\gamma_z}}\cos\theta_t.
\end{aligned} \tag{18}$$

Solving for $\mathcal{R}$ gives the equation for the reflection coefficient for a TM_y wave:

$$\mathcal{R} = \frac{\sqrt{\frac{\lambda_y}{\lambda_z}}\cos\theta_i - \sqrt{\frac{\gamma_y}{\gamma_z}}\cos\theta_t}{\sqrt{\frac{\lambda_y}{\lambda_z}}\cos\theta_r + \sqrt{\frac{\gamma_y}{\gamma_z}}\cos\theta_t}. \tag{19}$$

Taking the ratios of y-coordinates

$$\frac{\hat{y}\cdot\vec{H}_r}{\hat{y}\cdot\vec{H}_i} \quad \text{and} \quad \frac{\hat{y}\cdot\vec{H}_t}{\hat{y}\cdot\vec{H}_i}$$

to be constant on the interface $x = 0$ gives Snell's law:

$$\begin{aligned}
\sin\theta_i &= \sin\theta_r \\
\sqrt{\lambda_x\lambda_y}\sin\theta_i &= \sqrt{\gamma_x\gamma_y}\sin\theta_t.
\end{aligned} \tag{20}$$

A similar calculation shows that (19) and (20) are also the reflection coefficient and Snell's law for TE_y waves at the $x = 0$ interface.

Proposition 3.1. *Assume that $\mathcal{T} \neq 0$ and that*

$$\begin{aligned}
\lambda_y/\lambda_z &= \gamma_y/\gamma_z \\
\lambda_x\lambda_y &= \gamma_x\gamma_y.
\end{aligned} \tag{21}$$

Then equations (18) *and* (20) *imply that* $\mathcal{R} = 0$ *and there exist integers* n *and* m *such that*

$$\begin{aligned} \theta_r &= \theta_i + 2n\pi \\ \theta_t &= \theta_i + 2m\pi. \end{aligned} \tag{22}$$

Proof. By Snell's law (20) and the Pythagorean identity we must have $\cos\theta_i = \pm\cos\theta_r$ and $\cos\theta_i = \pm\cos\theta_t$. Since $\mathcal{T} \neq 0$ the linear equations (18) will have a finite solution if and only if $\cos\theta_i = \cos\theta_r = \cos\theta_t$. Consequently $\mathcal{R} = 0$ by (19) and $\sin(\theta_i - \theta_r) = \sin(\theta_i - \theta_t) = 0$ by standard trigonometric identities. The complex sine function has only real roots, so θ_i is related to θ_r and θ_t by (22).

Thus, if Λ^+ and Λ^- satisfy (21), the planar interface normal to the x-axis will be reflectionless, and the angles of incidence, reflection, and transmission will be the same for all plane waves. Similar results can be obtained for planar interfaces normal to the y-axis or z-axis.

4. Problem Formulation

In this section we give a problem geometry that allows for arbitrarily many PMLs, and for each PML we define the anisotropy matrix T in the constitutive relations (3). We show that the PML interfaces are reflectionless and that energy is attenuated in each PML. The variational equation (10) on each homogeneous region is used to formulate a global variational equation for E with the PML and polarization terms satisfying auxiliary differential equations. Finally, an absorbing boundary condition is placed on three sides of our computation domain to further damp the reflected energy.

Problem Geometry. We assume that E, P, and J_s in (10) are independent of y so our computational domain is contained in the xz-plane as depicted in Figure 2. Let X and Z be closed intervals in the respective x- and z-axes, and let $\mathcal{D} = X \times Z$ denote the computational domain.

We partition the intervals X into disjoint closed intervals X_-, X_0, and X_+ such that

$$\begin{aligned} \max X_- &= \min X_0 \\ \max X_0 &= \min X_+, \end{aligned}$$

and partition the interval Z into disjoint closed intervals Z_-, Z_v, and Z_d such that

$$\begin{aligned} \max Z_- &= \min Z_v \\ \max Z_v &= \min Z_d. \end{aligned}$$

The regions Z_v and Z_d are the vacuum and dielectric regions respectively. Let

$$Z_0 = Z_v \cup Z_d.$$

The region $X_0 \times Z_0$ will be our domain of interest. The buffer region $\mathcal{D} \setminus (X_0 \times Z_0)$ outside our domain of interest will contain the PMLs. This problem geometry is illustrated in Figure 2.

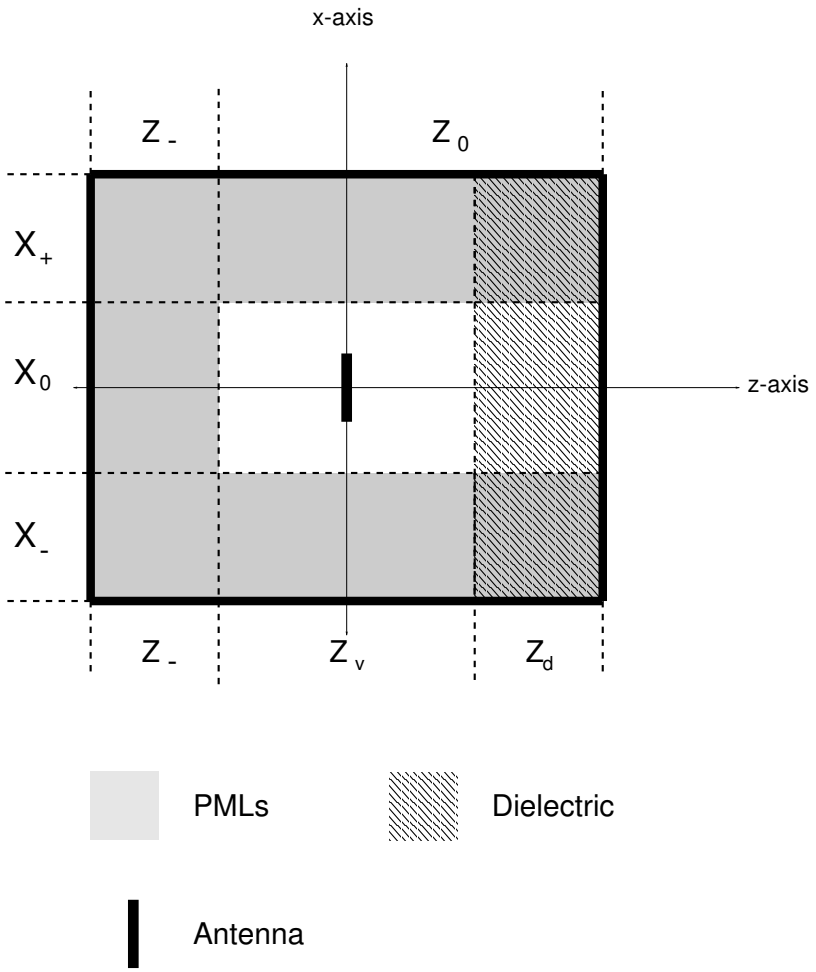

FIGURE 2. 2-D problem geometry

Perfectly Matched Layers. Let $\beta_x(x)$ and $\beta_z(z)$ be piecewise constant, convex functions such that $\beta_x = 0$ in X_0 and $\beta_z = 0$ in Z_0. The functions β_x and β_z control the damping in the PML regions. The convexity requirement implies that $\beta_x \geq 0$, $\beta_z \geq 0$ and that damping will be greater closer to the boundary of $\mathcal{D}$. Define

$$\begin{aligned} u_x(t,x) &= \delta(t) + \beta_x(x)\mathcal{H}(t) \\ u_z(t,z) &= \delta(t) + \beta_z(z)\mathcal{H}(t) \end{aligned} \tag{23}$$

where $\mathcal{H}$ is the Heaviside function. Let S_x and S_z be convolution operators on $C[0,\infty)$ with kernels u_x and u_z respectively. Then for fixed x and z, S_x and S_z are bijections on $C[0,\infty)$

since for any real β

$$(\delta(t) + \beta\mathcal{H}(t)) * (\delta(t) - \beta\mathcal{H}(t)e^{-\beta t}) = \delta(t).$$

Thus S_x, $S_z \in \mathcal{B}^+$ with $\mathcal{B}^+$ defined in (2).

On $X \times Z$ let the operator T in (3) be given by

$$T = \begin{pmatrix} S_x^{-1}S_z & 0 & 0 \\ 0 & S_xS_z & 0 \\ 0 & 0 & S_xS_z^{-1} \end{pmatrix}. \tag{24}$$

Although T is defined for a two-dimensional problem there is a straightforward generalization to three dimensions [9]. Our domain of interest is isotropic since S_x and S_z are the identity operator in the region $X_0 \times Z_0$.

The operator $\widetilde{T}$ defined in (5) is

$$\widetilde{T} = \operatorname{diag}(S_x^{-2}, I, S_z^{-2}) \tag{25}$$

where I is the identity operator.

We will show that the PML interfaces are reflectionless and that the PMLs attenuate energy. The operator Λ in (12) corresponding to (24) is

$$\Lambda = \begin{pmatrix} s_x^{-1}s_z & 0 & 0 \\ 0 & s_xs_z & 0 \\ 0 & 0 & s_xs_z^{-1} \end{pmatrix}$$

where

$$\begin{aligned} s_x &= 1 + \beta_x/(j\omega) \\ s_z &= 1 + \beta_z/(j\omega). \end{aligned} \tag{26}$$

Let $x = x_0$ be a point of discontinuity in β_x. Then the interface $x = x_0$ will be reflectionless by Proposition 3.1 since (21) is satisfied when

$$\begin{aligned} \Lambda^- = \operatorname{diag}(\lambda_x, \lambda_y, \lambda_z) &= \lim_{x \to x_0^-} \Lambda(x, z) \\ \Lambda^+ = \operatorname{diag}(\gamma_x, \gamma_y, \gamma_z) &= \lim_{x \to x_0^+} \Lambda(x, z). \end{aligned}$$

Consequently the reflection coefficient at the interface will vanish and each plane wave's angle of incidence equals its angle of transmission. Similar arguments show the interface at a discontinuity in β_z is also reflectionless with angle of incidence equaling angle of transmission for incident plane waves.

We can show that waves will be attenuated in each PML by introducing the transmitted wave vector $\vec{k}_t$ (17) into the plane wave solution (16). The plane wave's exponential term becomes

$$\exp\big(-jk_0\big(s_x(x)\cos(\theta_t)x + s_z(z)\sin(\theta_t)z\big)\big). \tag{27}$$

In PMLs matched to free space θ_t is real and the value k_0 defined in (14) is $k_0 = \omega/c$ where $c = 1/\sqrt{\epsilon_0\mu_0}$ is the wave speed. Thus by the definitions of s_x and s_z in (26) the absolute value of the exponential factor (27) is

$$\exp\big(-(1/c)(\beta_x(x)\cos(\theta_t)x + \beta_z(z)\sin(\theta_t)z)\big).$$

Thus in a PML matched to free space there is attenuation in the direction of wave propagation $\cos\theta_t\hat{x} + \sin\theta_t\hat{z}$, and the rate of attenuation in the x and z directions is controlled by the magnitudes of β_x and β_z respectively.

In the dielectric region $X \times Z_d$, $s_z = 1$ since $\beta_z = 0$ on Z_0, and the product $k_0\cos\theta_t$ in (27) is real-valued since planes of constant amplitude in the dielectric $X_0 \times Z_d$ are parallel to the xy-plane [2, pp. 210–212]. Thus in a PML matched to a dielectric the absolute value of the exponential factor (27) is

$$\exp\big(-(\beta_x(x)/\omega)k_0\cos(\theta_t)x)\ \exp((\Im(k_0\sin\theta_t))z).$$

Thus there is attenuation in the $+x$ and $-x$ directions in the PMLs matched to a dielectric, the magnitude of β_x controls the rate of attenuation, and the attenuation is frequency and direction dependent.

Auxiliary Differential Equations. We will next reformulate the variational equation (10) so that each PML term satisfies an auxiliary differential equation. Define V_x and V_z by

$$\begin{aligned} V_x + E &= \widetilde{T}_x E \\ V_z + E &= \widetilde{T}_z E. \end{aligned} \tag{28}$$

From (25) we have $\widetilde{T}_x = S_x^{-2}$. So by the definition of the kernel u_x of S_x in (23) we have

$$\begin{aligned} \ddot{E} &= \partial_t^2(\widetilde{T}_x)^{-1}(V_x + E) \\ &= \partial_t^2 S_x^2(V_x + E) \\ &= \partial_t^2(u_x * u_x) * (V_x + E) \\ &= (\ddot{\delta} + 2\beta_x\dot{\delta}(t) + \beta_x^2\delta) * (V_x + E) \\ &= \ddot{V}_x + \ddot{E} + 2\beta_x(\dot{V}_x + \dot{E}) + \beta_x^2(V_x + E). \end{aligned}$$

Thus by (28) we may replace the $\widetilde{T}_x E$ term in the variational equation (10) with $V_x + E$ and V_x satisfies the ordinary differential equation

$$\ddot{V}_x + 2\beta_x(\dot{V}_x + \dot{E}) + \beta_x^2(V_x + E) = 0.$$

Similarly, since $\widetilde{T}_z = S_z^{-2}$ we may replace $\widetilde{T}_z E$ in the variational equation (10) with $V_z + E$ where

$$\ddot{V}_z + 2\beta_z(\dot{V}_z + \dot{E}) + \beta_z^2(V_z + E) = 0.$$

We model the dielectric region $X \times Z_d$ as a Debye medium [3, pp. 11–12], so that the polarization term P will satisfy the differential equation

$$\tau\dot{P} + P = \epsilon_0\epsilon_d I_{Z_d} E \tag{29}$$

where I_{Z_d} is the indicator function on $X \times Z_d$, τ is the relaxation time constant, and ϵ_d is a constant measuring the difference between the static relative permittivity (when $\omega = 0$) and the relative permittivity ϵ_r.

From the preceding discussion it follows that the variational equation (10) in any region Ω where β_x and β_z are constant can be written as

$$\begin{aligned}(30)\quad \mu_0\epsilon_0\langle\epsilon_r\ddot{E},\phi\rangle + \mu_0\langle\ddot{P},\phi\rangle + \mu_0\langle\sigma\dot{E},\phi\rangle + \langle\partial_x(E+V_x),\partial_x\phi\rangle + \langle\partial_z(E+V_z),\partial_z\phi\rangle \\ - \langle\partial_x(E+V_x),n_x\phi\rangle_{\partial\Omega} - \langle\partial_z(E+V_z),n_z\phi\rangle_{\partial\Omega} = -\mu_0\langle\dot{J}_s,\phi\rangle.\end{aligned}$$

where the polarization and PML terms in (30) satisfy

$$\begin{aligned}\tau\dot{P} + P &= \epsilon_0\epsilon_d I_{Z_d}E \\ \ddot{V}_x + 2\beta_x\dot{V}_x + \beta_x^2V_x &= -2\beta_x\dot{E} - \beta_x^2E \\ \ddot{V}_z + 2\beta_z\dot{V}_z + \beta_z^2V_z &= -2\beta_z\dot{E} - \beta_z^2E.\end{aligned} \tag{31}$$

The zero initial conditions for our problem imply that V_z will be supported in $X \times Z_-$, V_x will be supported in $(X_- \times Z) \cup (X_+ \times Z)$, and P will be supported in $X \times Z_d$.

Global Variational Equation. Our source term $\vec{J}_s$ in (8) will model an antenna in free space, and we assume the signal is polarized with oscillations in the xz–plane only. Let

$$\begin{aligned}\vec{J}_s(t,x,z) &= I_{(0,t_f)}(t)I_{(-\bar{x},\,\bar{x})}(x)\delta(z)\sin(\omega t)\hat{x} \\ &= J_s(t,x,z)\hat{x}\end{aligned} \tag{32}$$

where $I_{(a,b)}$ is the indicator function on the interval (a,b), $(\pm\bar{x},0) \in X_0 \times Z_v$, ωt_f is an integral multiple of 2π, and J_s is defined in (9).

There are interfaces between PMLs at jumps in the PML parameters $\beta_x(x)$ and $\beta_z(z)$. By construction these PML interfaces are reflectionless. However, when the problem is discretized numerical reflections occur at PML interfaces. These numerical reflections can be made arbitrarily small by making the jumps in β_x and β_z sufficiently small.

We note that during a finite time interval $[0, t_{\text{final}}]$, the sum of the boundary integrals in (30), $\langle\partial_x(E+V_x),n_x\phi\rangle_{\partial\Omega}$ or $\langle\partial_z(E+V_z),n_z\phi\rangle_{\partial\Omega}$, that arise from both sides of a PML interface can be made arbitrarily small by taking the jumps in β_x and β_z to be sufficiently small. Comparison calculations we have performed with and without the boundary integrals from the PML interfaces (i.e., numerical computations including the integral terms properly with quadratures vs. approximating the net integral contributions by zero) reveal that these interface integral terms contribute very little to understanding the error control issues related to reflections at the interfaces of the dielectric relative to those at the boundaries of the finite computational domain. We have therefore, in this paper, chosen to approximate the interface integrals by zero in our calculations, simplifying and concentrating on the reflections from the computational boundary and the vacuum-dielectric interface. Other calculations (not reported here) verify that the conclusions of our results with respect to inverse problem methodology are not altered by inclusion of the PML interface integral terms in our system.

After approximating the sum of the boundary integrals from both sides of a PML interface by zero we obtain a variational equation that will hold on the entire domain $\mathcal{D}$:

$$\begin{aligned}(33)\quad \mu_0\epsilon_0\langle\epsilon_r\ddot{E},\phi\rangle + \mu_0\langle\ddot{P},\phi\rangle + \mu_0\langle\sigma\dot{E},\phi\rangle + \langle\partial_x(E+V_x),\partial_x\phi\rangle + \langle\partial_z(E+V_z),\partial_z\phi\rangle \\ - \langle\partial_x(E+V_x),n_x\phi\rangle_{\partial\mathcal{D}} - \langle\partial_z(E+V_z),n_z\phi\rangle_{\partial\mathcal{D}} = -\mu_0\langle\dot{J}_s,\phi\rangle.\end{aligned}$$

where the polarization and PML terms satisfy (31).

Absorbing Boundary Condition. We next add boundary conditions to our problem formulation. Let C_{-x}, C_{+x}, C_{-z}, and C_{+z} denote the four boundaries of $\mathcal{D}$ with outward normals in the $-x$, $+x$, $-z$ and $+z$ directions respectively. Assign the boundary conditions

$$\begin{aligned}(\beta_x+\partial_t)E &= c\partial_x E \qquad \text{on } C_{-x}\\ (\beta_x+\partial_t)E &= -c\partial_x E \qquad \text{on } C_{+x}\\ (\beta_z+\partial_t)E &= c\partial_z E \qquad \text{on } C_{-z}\\ E &= 0 \qquad \text{on } C_{+z}\end{aligned} \tag{34}$$

where $c = 1/\sqrt{\mu_0\epsilon_0}$. The boundary condition on C_{+z} models a dielectric with a supraconductive backing. We show below that the remaining three boundary conditions are absorbing boundary conditions for PMLs matched to free space.

Take an incident plane wave on the C_{+x} boundary with the form

$$E_i = \exp(-jk_0(s_x(x)\cos(\theta_i)x + s_z(z)\sin(\theta_i)z))\exp(j\omega t).$$

Then the reflected wave will have the form

$$E_r = \mathcal{R}\exp(-jk_0(-s_x(x)\cos(\theta_i)x + s_z(z)\sin(\theta_i)z))\exp(j\omega t).$$

The total wave is $E = E_i + E_r$.

For PMLs matched to free space, θ_i is real-valued and

$$k_0\cos(\theta_i) = (\omega/c)\cos(\theta_i)$$

by (14). For PMLs matched to the dielectric, we may assume the plane wave traveled across the vacuum–dielectric interface. Applying Snell's law at the vacuum-dielectric interface shows that $k_0\cos(\theta_i)$ is real-valued [2, pp. 210–212] and

$$k_0\cos(\theta_i) = (\omega/c)\cos(\widetilde{\theta}_i)$$

where $\widetilde{\theta}_i$ is the real-valued angle of incidence on the vacuum-dielectric interface. Let $\theta = \theta_i$ for PMLs matched to free space and $\theta = \widetilde{\theta}_i$ for PMLs matched to the dielectric. Then applying the boundary condition $(\beta_x+\partial_t)E = -c\partial_x E$ on C_{+x} leads to the equality

$$\begin{aligned}(\beta_x+j\omega)(1+\mathcal{R}) &= c(js_x\omega/c)\cos(\theta)(1-\mathcal{R})\\ &= j\omega(1+\beta_x/(j\omega))\cos(\theta)(1-\mathcal{R})\\ &= (\beta_x+j\omega)\cos(\theta)(1-\mathcal{R}).\end{aligned}$$

Solving for $\mathcal{R}$ gives

$$\mathcal{R} = \frac{\cos\theta - 1}{\cos\theta + 1} \tag{35}$$

where θ is a real-valued angle of incidence for either the boundary C_{-x} or the vacuum-dielectric interface. Similarly one can also show that (35) is the reflection coefficient for the boundary conditions (34) on C_{-x} and C_{-z}.

Thus the reflection coefficient $\mathcal{R}$ depends on an angle of incidence and is independent of the frequency. The reflection coefficient vanishes for $\theta = 0$ and $|\mathcal{R}|$ is an increasing function of θ on $(0, \pi/2)$. In our problem we can generally expect $\theta \leq \pi/4$. Reflected waves with sufficiently large angles of incidence will reflect off two boundaries before returning to the domain of interest. Consequently, it is reasonable to expect this absorbing boundary condition will reflect approximately

$$\left(\frac{\cos(\pi/4) - 1}{\cos(\pi/4) + 1}\right)^2 = 0.03$$

of the energy. This shows that the absorbing boundary condition plays a useful role in damping outgoing energy. Indeed, unlike the situation suggested in [12], the absorbing boundary conditions combined with the PMLs can enhance energy absorption. Our comparison calculations have verified this, at least for the problems considered in this paper.

Since differentiation commutes with convolution, it follows from the definitions of V_x and V_z in (28) that the same boundary conditions will hold with V_x and V_z replacing E. Thus the variational equation (33) becomes

$$\begin{aligned}\mu_0\epsilon_0\langle\epsilon_r\ddot{E},\phi\rangle + \mu_0\langle\ddot{P},\phi\rangle + \mu_0\langle\sigma\dot{E},\phi\rangle + \langle\partial_x(E+V_x),\partial_x\phi\rangle + \langle\partial_z(E+V_z),\partial_z\phi\rangle \\ + \langle(1/c)(\beta_x+\partial_t)(E+V_x),\phi\rangle_{C_{-x}\cup C_{+x}} + \langle(1/c)(\beta_z+\partial_t)(E+V_z),\phi\rangle_{C_{-z}} = -\mu_0\langle\dot{J}_s,\phi\rangle.\end{aligned} \tag{36}$$

5. Discretization

To aid the numerical calculations we scale the time variable by a factor of $c = 1/\sqrt{\epsilon_0\mu_0}$ so that $\dot{E}$ is replaced by $c\dot{E}$, $\dot{P}$ is replaced by $c\dot{P}$, etc., and we scale the polarization P by a factor of $1/\epsilon_0$ so that P is replaced by $\epsilon_0 P$. The variational equation (36) becomes

$$\begin{aligned}\langle\epsilon_r\ddot{E},\phi\rangle + \langle\ddot{P},\phi\rangle + \eta_0\langle\sigma\dot{E},\phi\rangle + \langle\partial_x(E+V_x),\partial_x\phi\rangle + \langle\partial_z(E+V_z),\partial_z\phi\rangle \\ + \langle(\alpha_x+\partial_t)(E+V_x),\phi\rangle_{C_{-x}\cup C_{+x}} + \langle(\alpha_z+\partial_t)(E+V_z),\phi\rangle_{C_{-z}} = -\eta_0\langle\dot{J}_s,\phi\rangle\end{aligned} \tag{37}$$

where $\eta_0 = \sqrt{\mu_0/\epsilon_0}$ is the impedance of free space, $\alpha_x = \beta_x/c$, and $\alpha_z = \beta_z/c$.

The differential equations (31) become

$$\begin{aligned}\dot{P} + \gamma P &= \epsilon_d\gamma I_{Z_d} E \\ \ddot{V}_x + 2\alpha_x\dot{V}_x + \alpha_x^2 V_x &= -2\alpha_x\dot{E} - \alpha_x^2 E \\ \ddot{V}_z + 2\alpha_z\dot{V}_z + \alpha_z^2 V_z &= -2\alpha_z\dot{E} - \alpha_z^2 E\end{aligned} \tag{38}$$

with $\gamma = (c\tau)^{-1}$.

After scaling our source term (32) in the time variable, we obtain

$$J_s(t,x,z) = I_{(0,t_f)}(t/c) I_{(-\bar{x},\,\bar{x})}(x)\delta(z)\sin((\omega/c)t) \tag{39}$$

where $(\omega/c)t_f$ is an integral multiple of 2π.

We will use a Galerkin finite element approximation to discretize the problem in the spatial variable to obtain piecewise linear approximates for $E(t,\cdot)$ and $P(t,\cdot)$. Choose strictly increasing sequences of real numbers

$$\Pi_x = \{x_i\}_{i=1}^{N_x} \subset X$$
$$\Pi_z = \{z_j\}_{j=1}^{N_z} \subset Z$$

such that Π_x contains the end points of X and such that Π_z contains the end points of Z and Z_d. Our grid will be the Cartesian product

$$\mathcal{G} = \{(x,z) : x \in \Pi_x,\ z \in \Pi_z\}, \tag{40}$$

and the vacuum-dielectric boundary will coincide with a line of grid points. We then construct a triangulation $\mathcal{T}$ of the computational region $\mathcal{D}$ such that for each triangle $\tau \in \mathcal{T}$, the set of vertices $v(\tau)$ satisfies

$$v(\tau) = \{(x_i, z_j),\ (x_i, z_{j+1}),\ (x_{i+1}, z_{j+1})\}$$

or

$$v(\tau) = \{(x_i, z_j),\ (x_{i+1}, z_j),\ (x_{i+1}, z_{j+1})\}$$

for some $1 \le i < N_x$ and $1 \le j < N_z$.

Since $E = 0$ on C_{+z}, let $\{q_j\}_{j=1}^{N}$ be an enumeration of the $N = N_x N_z - (N_x - 2)$ grid points lying in $\mathcal{D}$ that are not in the interior C_{+z} and let $\{\phi_i(x,z)\}_{i=1}^{N}$ be the standard piecewise linear spline functions that are linear on each triangle $\tau \in \mathcal{T}$ and satisfy

$$\phi_i(q_j) = \begin{cases} 1 & i = j \\ 0 & i \neq j. \end{cases}$$

Then we can approximate E, P, V_x, and V_z with

$$\begin{aligned} E(t,x,z) &\approx \sum_{j=1}^{N} e_j(t)\phi_j(x,z) \\ P(t,x,z) &\approx \sum_{j=1}^{N} p_j(t)\phi_j(x,z) \\ V_x(t,x,z) &\approx \sum_{j=1}^{N} (v_x)_j(t)\phi_j(x,z) \\ V_z(t,x,z) &\approx \sum_{j=1}^{N} (v_z)_j(t)\phi_j(x,z). \end{aligned} \tag{41}$$

The basis functions ϕ_j and the coefficient functions e_j, p_j, $(v_x)_j$, and $(v_z)_j$ depend on the chosen grid $\mathcal{G}$. Let e, p, v_x, and v_z be N-dimensional vectors formed from these coefficient functions (e.g., $e = (e_1, e_2, \ldots, e_N)^T$).

If $\phi = \sum_{j=1}^{N} c_j\phi_j$, then we will approximate $\alpha_x(x)\phi(x,z)$ and $\alpha_z(z)\phi(x,z)$ with

$$\begin{aligned} \alpha_x\phi &\approx \sum_{j=1}^{N} \alpha_x(x(q_j))c_j\phi_j \\ \alpha_z\phi &\approx \sum_{j=1}^{N} \alpha_z(z(q_j))c_j\phi_j. \end{aligned} \tag{42}$$

where $x(q_j)$ and $z(q_j)$ denote the x and z coordinates of q_j.

Making the substitution $\phi = \phi_i$ and using the approximations (41) and (42) in the variational equation (37) and the differential equations (38), we obtain a Galerkin finite-dimensional system of equations

$$\begin{aligned} &(M + M_{Z_d}(\epsilon_\infty - 1))\ddot{e} + M_{Z_d}\ddot{p} + (L_x + A_xB_x)v_x + (L_z + A_zB_z)v_z \\ &\quad + (L_x + L_z + A_xB_x + A_zB_z)e + B_x\dot{v}_x + B_z\dot{v}_z + (B_x + B_z + \eta_0\sigma M_{Z_d})\dot{e} = \mathcal{J} \end{aligned} \tag{43}$$

with the polarization and PML terms satisfying

$$\begin{aligned} \dot{p} + \gamma p &= \epsilon_d\gamma I_d e \\ \ddot{v}_x + 2A_x\dot{v}_x + A_x^2 v_x &= -2A_x\dot{e} - A_x^2 e \\ \ddot{v}_z + 2A_z\dot{v}_z + A_z^2 v_z &= -2A_z\dot{e} - A_z^2 e \end{aligned} \tag{44}$$

where ϵ_∞ is the relative permittivity in the dielectric and

$$
\begin{aligned}
M_{i,j} &= \langle \phi_j, \phi_i \rangle \\
(M_{Z_d})_{i,j} &= \langle I_{Z_d}\phi_j, \phi_i \rangle \\
(L_x)_{i,j} &= \langle \partial_x \phi_j, \partial_x \phi_i \rangle \\
(L_z)_{i,j} &= \langle \partial_z \phi_j, \partial_z \phi_i \rangle \\
(B_x)_{i,j} &= \langle \phi_j, \phi_i \rangle_{C_{-x} \cup C_{+x}} \\
(B_z)_{i,j} &= \langle \phi_j, \phi_i \rangle_{C_{-z}} \\
(A_x)_{i,j} &= \begin{cases} \alpha_x(x(q_j)) & i = j \\ 0 & i \neq j \end{cases} \\
(A_z)_{i,j} &= \begin{cases} \alpha_z(z(q_j)) & i = j \\ 0 & i \neq j \end{cases} \\
(I_d)_{i,j} &= \begin{cases} 1 & i = j \text{ and } I_{Z_d}\phi_i \neq 0 \\ 0 & \text{otherwise} \end{cases} \\
\mathcal{J}_i &= -\eta_0 \langle \dot{J}_s, \phi_i \rangle.
\end{aligned} \tag{45}
$$

We replace the $M_{Z_d}\ddot{p}$ term in (43) by using the differential equation and its derivative for P in (44) to obtain

$$M_{Z_d}\ddot{p} = \gamma^2 M_{Z_d} p + \epsilon_d \gamma M_{Z_d}\dot{e} - \epsilon_d \gamma^2 M_{Z_d} e.$$

The final form of our variational equation is

$$
\begin{aligned}
(M + M_{Z_d}(\epsilon_\infty - 1))\ddot{e} + \gamma^2 M_{Z_d} p + (L_x + A_x B_x)v_x + (L_z + A_z B_z)v_z \\
+ (L_x + L_z + A_x B_x + A_z B_z - \epsilon_d \gamma^2 M_{Z_d})e + B_x \dot{v}_x + B_z \dot{v}_z \\
+ (B_x + B_z + (\eta_0 \sigma - \epsilon_d \gamma) M_{Z_d})\dot{e} = \mathcal{J}
\end{aligned} \tag{46}
$$

with the polarization and PML terms satisfying (44).

The resulting system of equations can be written as a first order system in the composite variable

$$\xi = (p, v_x, v_z, e, \dot{v}_x, \dot{v}_z, \dot{e})^T,$$

and we approximate a solution to this system using the Crank–Nicholson scheme [3, pp. 58–60].

6. Numerical Results

In this section we present numerical results which show that PMLs attenuate energy and that numerical reflections from the PML interfaces can be controlled.

For these simulations the conductivity is $\sigma = 1.0 \times 10^{-2}$, and the Debye parameters in the differential equation (29) are $\tau = 1.0 \times 10^{-11}$ and $\epsilon_d = 30.0$. The relative permittivity in the

dielectric is $\epsilon_\infty = 5.0$. The antenna is centered at the origin, and the interrogating signal (39) will have 3 cycles. The source term parameters in (39) are

$$\begin{aligned} \bar{x} &= 0.03 \\ \omega &= 2\pi \times 1.8 \times 10^9 \text{ rad/sec} \\ t_f &= 6\pi c/\omega \quad (\approx 0.5 \text{ sec}). \end{aligned}$$

The time step for the finite differencing is 1.0×10^{-4} units in the scaled time variable.

We define the following sequence to discretize our PML regions: $\xi_0 = 0.05$ and

$$\xi_j = \xi_{j-1} + (0.0025) + \frac{j-1}{59}(0.0125) \qquad j = 1, 2, \ldots 60.$$

For the PML parameters let $\alpha_0 = 0.0$ and

$$\alpha_j = \alpha_{j-1} + (0.01) + \frac{j-1}{59}(0.11) \qquad j = 1, 2, \ldots 60. \tag{47}$$

Let

$$\begin{aligned} X_- &= [-\xi_{60}, -\xi_0] & Z_- &= [-\xi_{60}, -\xi_0] \\ X_0 &= [-0.05, 0.05] & Z_v &= [-0.05, 0.05] \\ X_+ &= [\xi_0, \xi_{60}] & Z_d &= [0.05, 0.35]. \end{aligned}$$

Our grid $\mathcal{G}$ will be the Cartesian product

$$\mathcal{G} = \{(x, z) : \ x \in \Pi_- \cup \Pi_v \cup \Pi_+, \ z \in \Pi_- \cup \Pi_v \cup \Pi_d\}$$

where

$$\begin{aligned} \Pi_v &= \{(0.0025)j : -20 \le j \le 20\} \\ \Pi_d &= \{(0.0025)j : 20 \le j \le 140\} \\ \Pi_+ &= \{\xi_j : 0 \le j \le 60\} \\ \Pi_- &= \{-\xi_j : 0 \le j \le 60\}. \end{aligned}$$

Let $\alpha_x(\xi)$ be any piecewise constant, convex function satisfying $\alpha_x = 0$ on X_0 and $\alpha_x(\xi_j) = \alpha_x(-\xi_j) = \alpha_j$. Let α_z be any piecewise constant, convex function satisfying $\alpha_z = 0$ on $Z_0 = Z_v \cup Z_d$ and $\alpha_z(-\xi_j) = \alpha_j$.

There will be a loss in accuracy due to the coarser grid as we approach the boundary of $\mathcal{D} = X \times Z$, but the coarser grid occurs outside of our domain of interest and substantially reduces the number of grid nodes needed for our simulation.

The interfaces between PMLs are reflectionless; however, when the problem is discretized numerical reflections occur when there are jumps in the PML parameter. These numerical reflections at a PML interface may be made arbitrarily small by making the jump in the PML parameters α_j sufficiently small.

We have also computed the solution when the grid $\mathcal{G}$ is preserved and the PMLs are replaced with free space. The absolute difference between the free space solution and the PML solution in the domain of interest $X_0 \times Z_0$ is less than 0.6. By contrast, the amplitude of

the signal after reflecting off the vacuum-dielectric interface is approximately 15 as we will see in Figure 3. This implies that the error in the domain of interest due to numerical reflections from the PMLs is less than $0.6/15 = 4\%$ of the amplitude of the reflected interrogating signal.

In Figures 3, 4, and 5 we give snapshots $E(\tilde{t}, 0, z)$ of the electric field along the z-axis at times $\tilde{t} = 0.6001$, 1.6001, and 3.6000, respectively.

The source current J_s propagates three cycles during the time interval $0 < t < t_f \approx 0.5$, and energy travels at unit speed in the vacuum region $-0.05 < z < 0.05$ and the PML region $z < -0.5$. Consequently at time $t = 0.6001$ (Figure 3) part of the original signal (the left moving part: the antenna emits both left and right moving interrogating signals into the vacuum) will be in the z-interval $(-0.6, -0.1)$, the signal reflected from the vacuum-dielectric interface at $z = 0.05$ will be in the z-interval $(-0.5, 0)$, and the transmitted signal will be in the dielectric region $0.05 < z < .35$. The trailing wave crest of the reflected signal is visible at $z = 0$ and has an amplitude of approximately 15. The PML induced damping of the signal is evident in the PML region $z < -0.05$.

At time $t = 1.6001$ (Figure 4) the Brillouin precursors [1, 3, 8] can be seen in the Debye medium $0.05 < z < 0.35$. The signal in the Debye medium is still moving in the positive z direction. The original left-moving signal and the signal reflected from the vacuum-dielectric interface have had sufficient time to hit the computational boundary and return to the domain of interest $X_0 \times Z_0$. All the energy evident in the vacuum interval $-0.05 < z < 0.05$ has returned after reflecting off a PML interface or the computational boundary. The amplitude of this reflected energy is less than 0.4 while the amplitude of the leading wave crest in the dielectric is approximately 1.6.

At time $t = 3.6$ (Figure 5) the transmitted signal has reflected off the dielectric's supraconductive backing and has emerged from the dielectric. The leading wave crest of this secondary reflection is visible at $z = 0$. The energy that has returned to the domain of interest $X_0 \times Z_0$ after reflecting off a PML interface or the computational boundary is seen as "saw teeth" superposed on the leading wave crest of the secondary reflection off the dielectric's supraconductive backing. This figure shows that the depth of the dielectric material is recoverable in the inverse problem (see [3] for details on how this is done).

The amount of numerical reflection from the PML interfaces can be controlled by making the jumps in the PML parameters sufficiently small. For instance, if the PML parameters α_j in (47) are redefined to be

$$\alpha_j = \alpha_{j-1} + (0.001) + \frac{j-1}{59}(0.011) \qquad\qquad j = 1, 2, \ldots 60.$$

then a simulation shows that the error in the domain of interest due to numerical reflections from the PMLs is less than 0.08. (As mentioned above, the PML parameters in (47) give a maximum error of 0.6.) However, the damping in the PML region is much less with these smaller parameters. If smaller jumps in the PML parameter are used then more grid points are needed in the regions X_-, X_+, and Z_- to obtain the damping achieved using larger jumps.

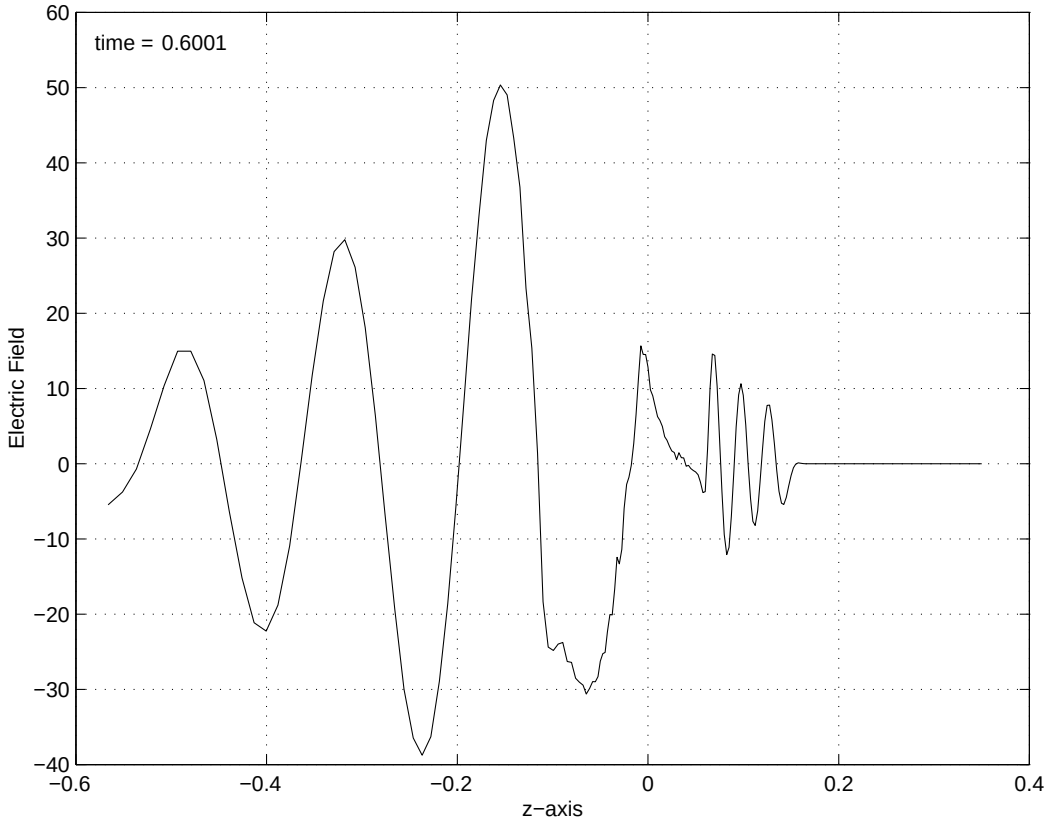

FIGURE 3. Graph of $E(0.6001,\, 0,\, z)$ for $z \in Z$

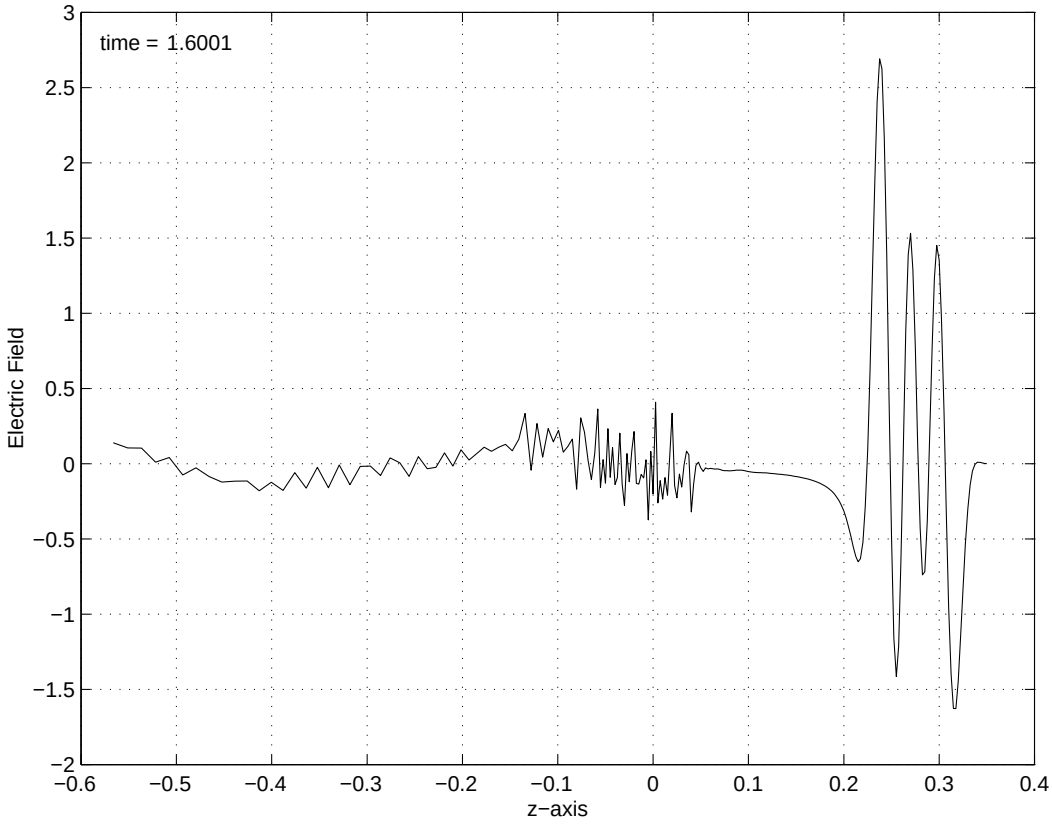

FIGURE 4. Graph of $E(1.6001, 0, z)$ for $z \in Z$

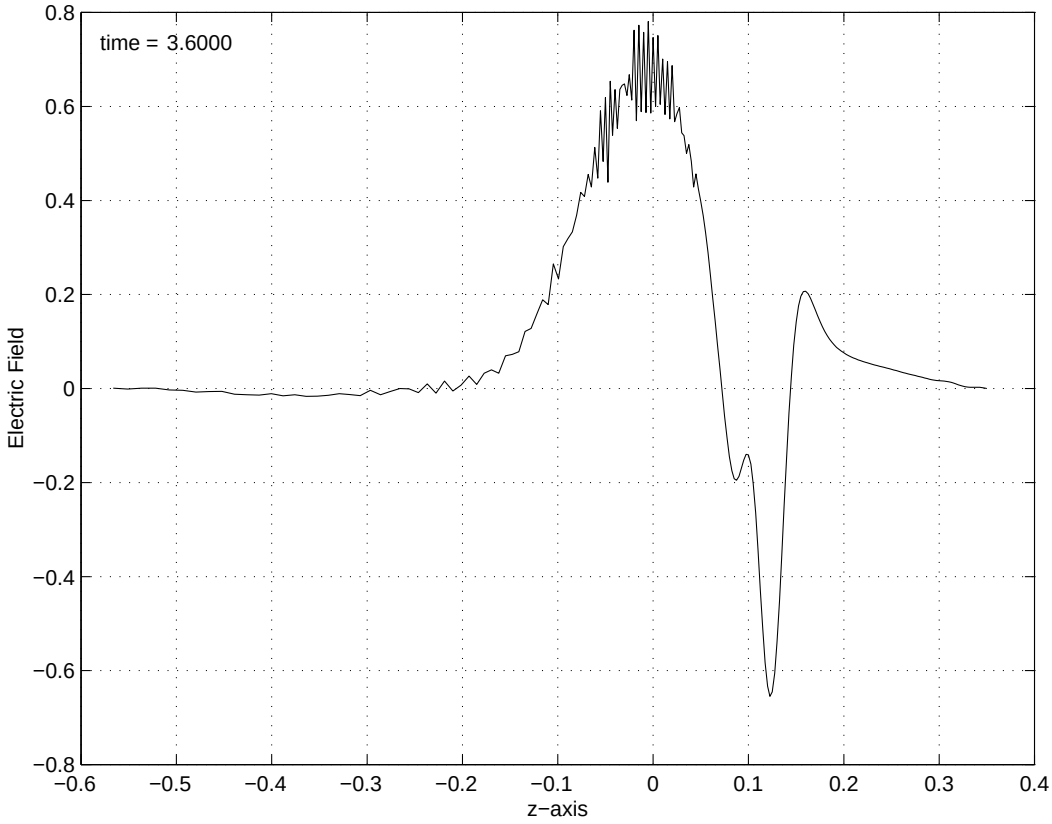

FIGURE 5. Graph of $E(3.6,\, 0,\, z)$ for $z \in Z$

7. Concluding Remarks

Numerical simulations demonstrate that reflections from interfaces at PML boundaries can be controlled by reducing the number or magnitude of the jumps in the PML parameter. Furthermore, our simulations have demonstrated that attenuation occurs in the PML regions, so expanding the size of PML regions results in greater energy attenuation. Thus a strategy of reducing the size and number of jumps in the PML parameter while expanding the size of the PML regions will allow one to simultaneously control both the reflection from PML interfaces and the return of energy from the computational boundary.

The successful use of PMLs in these simulations enables us to compute the electromagnetic field and solve a 2-D forward problem while controlling reflections from finite computational domains. We fully anticipate that our solution methodology for the forward problem will

permit us to determine dielectric depth and parameters in an inverse problem thereby extending the inverse problem methodology for the one-dimensional case given in [3]. We are currently combining the ideas presented here with a reduced order computational methodology (Proper Orthogonal Decomposition based techniques, see [4] for details) in pursuing multidimensional domain inverse problems that generalize to higher dimensions the ideas of [3].

8. Acknowledgments

The authors are grateful to Richard Albanese for numerous discussions and frequent encouragement. This research was partially supported by the U. S. Air Force Office of Scientific Research under grant AFOSR F49620-01-1-0026.

References

[1] Richard Albanese, John Penn, and Richard Medina. Short-rise-time microwave pulse propagation through dispersive biological media. *J. Optical Society of America A*, 6(9):1441–1446, 1989.
[2] Constantine A. Balanis. *Advanced Engineering Electromagnetics*. John Wiley & Sons, New York, 1989.
[3] H. T. Banks, M. W. Buksas, and T. Lin. *Electromagnetic Material Interrogation Using Conductive Interfaces and Acoustic Wavefronts*. SIAM, Philadelphia, 2000.
[4] H. T. Banks and G. M. Kepler. Reduced order computational methods for electromagnetic material interrogation using pulsed signals and conductive reflecting interfaces. *J. Inverse and Ill-posed Problems*, 11(4), 2003.
[5] Jean-Pierre Berenger. A perfectly matched layer for the absorption of electromagnetic waves. *J. Comput. Physics*, 114(2):185–200, 1994.
[6] J. G. Blaschak and J. Franzen. Precursor propagation in dispersive media from short-rise-time pulses at oblique incidence. *J. Optical Society of America A*, 12:1501–1512, 1995.
[7] V. A. Bokil and M. W. Buksas. A 2D mixed finite element formulation of the uniaxial perfectly matched layer. *J. Comput. Physics, submitted*.
[8] L. Brillouin. *Wave Propagation and Group Velocity*. Academic Press, New York, 1960.
[9] M. W. Buksas. Implementing the perfectly matched layer absorbing boundary condition with mimetic differenceing schemes. In F. L. Teixeira, editor, *Geometric Methods for Computational Electromagnetics*, number 32 in Progress in Electromagnetic Research Series, pages 383–411. EMW Publishing, Cambridge, Mass., 2001.
[10] Bjorn Engquist and Andrew Majda. Absorbing boundary conditions for the numerical simulation of waves. *Mathematics of Computation*, 31(139):629–651, 1977.
[11] F. G. Friedlander. *Introduction to the Theory of Distributions*. Cambridge University Press, Cambridge, 1982.
[12] P. G. Petropoulos. On the termination of the perfectly matched layer with local absorbing boundary conditions. *J. Comput. Physics*, 143:665–673, 1998.
[13] Zachary S. Sacks, David M. Kingsland, Robert Lee, and Jim-Fee Lee. A perfectly matched anisotropic absorber for use as an absorbing boundary condition. *IEEE Trans. Antennas Propagat.*, 43(12):1460–1463, December 1995.
[14] E. Turkel and A. Yefet. Absorbing PML boundary layers for wave-like equations. *Appl. Num. Math.*, 27:533–557, 1998.
[15] R. W. Ziolkowski. Time-derivative Lorentz material model-based absorbing boundary condition. *IEEE Trans. Antennas Propagation*, 45:1530–1535, 1997.

Current address, Brian L. Browning: GlaxoSmithKline, Five Moore Drive, Research Triangle Park, NC 27709, USA